Coordination Chemistry Reviews, 93 (1989) 19–57
Elsevier Science Publishers B.V., Amsterdam – Printed in The Netherlands

APPLICATION OF HIGH PRESSURE KINETIC TECHNIQUES TO MECHANISTIC STUDIES IN COORDINATION CHEMISTRY

M. KOTOWSKI and R. van ELDIK *

Institute for Inorganic Chemistry, University of Witten/Herdecke, Stockumerstrasse 10, 5810 Witten (F.R.G.)

(Received 17 March 1988)

CONTENTS

A. INTRODUCTION

It is the general objective of kinetic studies to elucidate the mechanism of a chemical reaction and to contribute to our understanding of the chemical process on a molecular level. Such measurements usually involve the determination of reaction rates and rate constants as a function of many chemical and physical parameters in order to formulate an empirical rate law that describes the behaviour of the chemical reaction under all conditions investigated. The variables usually studied include the concentration of reactant and product species, pH, solvent, ionic strength and temperature. Much emphasis is usually placed on the meaning of the activation parame-

* Author to whom all correspondence should be addressed.

0010-8545/89/$13.65

ters $\Delta H^{\ddagger}$ and $\Delta S^{\ddagger}$ obtained from the temperature dependence of the process. The accuracy of the reaction mechanism suggested is likely to increase with the increasing number of variables covered during such investigations. This is one of the reasons why, in an increasing number of studies over the past decade, the additional variable of pressure has been included as a kinetic or thermodynamic parameter. Such additional information may not only assist in the elucidation of the intimate nature of the reaction mechanism, but may also reveal fundamental aspects of the systems studied. It may also improve our comprehension of the reaction kinetics by adding a kinetic parameter which the suggested mechanism must also take into consideration. In this respect, it is important to realize that pressure is a fundamental physical variable that can affect various thermodynamic and kinetic parameters. It is therefore a variable at least as or even more powerful than the more generally applied variable of temperature.

Pressure can be varied over a wide range and applied to many different chemical problems [1–3]. The pressure range varies from a few to hundreds of kilobars (1 kbar = 100 MPa) depending on the technique employed and the phenomenon investigated. Pressures up to 100 kbar are in many cases required to induce structural changes and phase transitions. For kinetic and synthetic purposes in coordination chemistry the pressure range is usually limited to 400 MPa. In this range, no major changes in molecular dimensions, solvation numbers, electronic properties etc. are expected, and the observed effect is solely kinetic. Pressures up to 300 MPa can significantly affect the value of a rate or equilibrium constant, which forms the basis of all treatments of activation and reaction volume data. These quantities are interrelated in the case of volume profile treatments or in systems where pre-equilibria or acid–base equilibria exhibit a characteristic pressure dependence and form an integral part of the overall reaction mechanism.

When the rate of a process can be substantially affected by applying pressures up to 400 MPa, then this effect can be applied to synthetic purposes. This is especially true in processes where different reaction products are produced in parallel reaction paths that exhibit different pressure dependences.

Many reviews have appeared in recent years describing the effect of pressure on the reactions of inorganic and organometallic coordination compounds [4–19]. It is not the objective of this paper to present another review of this topic, since that is surely not needed at the present time. However, in terms of a special issue of this journal devoted to new techniques in coordination chemistry, it is appropriate to focus on the high pressure kinetic technique itself. It is our intention to demonstrate by using selected examples in coordination chemistry how this technique can be used to obtain additional and in many cases unique mechanistic information.

This paper is therefore in no way a review of the coordination chemistry studied using this technique, and readers are advised to consult the cited reviews [1–19] for detailed information. This paper will, however, present a review as complete as possible regarding the techniques used in such studies, an aspect which has not been treated in detail before.

The idea of performing experiments at high pressure usually invokes a fear of complicated, dangerous and expensive instrumentation. We hope that this review will demonstrate the opposite, namely that the instrumentation is rather simple, minimal dangers are involved with liquid phase systems at pressures up to 400 MPa, and that most of the instrumentation described is commercially available or can be manufactured by instrument shops. Thus kineticists should be encouraged to apply these techniques in future mechanistic studies to the same extent that temperature is used as a physical parameter.

B. FUNDAMENTAL PRINCIPLES

In almost all kinetic studies in the liquid phase, the interpretation of the pressure dependence of a rate constant is based on a simplified version of the transition state theory, which does not take the dynamics of the reactant–solvent interaction into account. This simplification usually applies to non-diffusion-controlled processes and has been adopted in the examples presented here. Possible modifications of the transition state theory, on the basis of high pressure kinetic data as a function of solvent [20,21], are treated elsewhere [22].

For a reaction of the type outlined in reaction (1), the simplest conceivable mechanism according to the transition state theory can be formulated as in reaction (2):

$$A + B \rightarrow AB \tag{1}$$

$$A + B \rightleftharpoons [A \cdots B]^{\ddagger} \rightarrow AB \tag{2}$$

A possible volume profile is given in Fig. 1. The magnitude and sign of the reaction volume, $\Delta\overline{V} = \overline{V}_{AB} - \overline{V}_{A} - \overline{V}_{B}$, and of the activation volume, $\Delta V^{\ddagger} = \overline{V}_{\ddagger} - \overline{V}_{A} - \overline{V}_{B}$, depend on the nature of the chemical species involved and their solvent environment. Such a profile is a pictorial view of the chemical process on the basis of volume changes. The reaction volume may be measured directly by dilatometry, or calculated from the partial molar volumes of the reactant and product species, determined from density measurements. Certainly, $\Delta\overline{V}$ can also be obtained from the pressure dependence of the overall equilibrium constant K for reaction (1) as shown in eqn. (3):

$$(\partial \ln K/\partial P)_{T} = -\Delta\overline{V}/RT \tag{3}$$

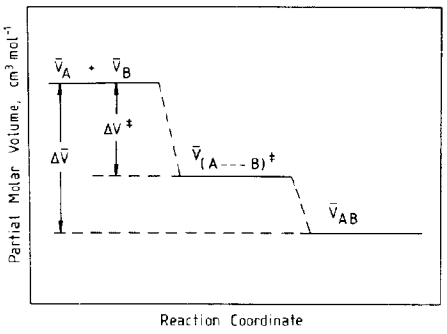

Fig. 1. Volume profile for the reaction $A + B \rightleftharpoons (A \cdots B)^{\ddagger} \rightarrow AB$.

In contrast, $\Delta V^{\ddagger}$ can only be determined from the pressure dependence of the rate constant k for reaction (1) as indicated in eqn. (4):

$$(\partial \ln k/\partial P)_T = -\Delta V^{\ddagger}/RT \tag{4}$$

The dependence of ln K (or ln k) on P is often found to be non-linear, indicating that $\Delta \bar{V}$ (or $\Delta V^{\ddagger}$) is a function of pressure. Various mathematical descriptions have been proposed for the treatment of such data, and details are given elsewhere [4,23]. Among these, perhaps the most popular is the parabolic function (eqn. (5)) for which $\Delta V^{\ddagger}$ at $P = 0$, i.e. $\Delta V_0^{\ddagger}$, is equal to $-bRT$, and $\Delta\beta^{\ddagger}$, defined as $-(\partial \Delta V^{\ddagger}/\partial P)_T$, is equal to $2cRT$:

$$\ln k = a + bP + cP^2 \tag{5}$$

$\Delta\beta^{\ddagger}$ represents the compressibility coefficient of activation, a measure of the pressure dependence of $\Delta V^{\ddagger}$. This parameter usually has a meaningful value in cases where the reaction is accompanied by significant solvational changes.

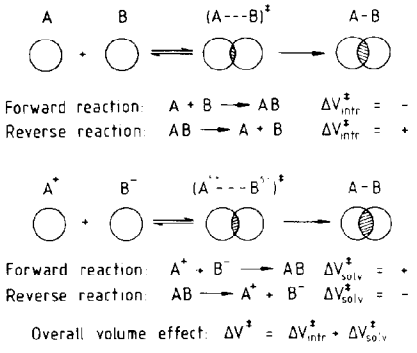

Fig. 2. Schematic representation of the sign and components of $\Delta V^{\ddagger}$ [3].

In general, the experimentally derived $\Delta V^{\ddagger}$ can be expressed as the sum of two contributions: $\Delta V^{\ddagger}_{intr}$, the intrinsic volume change associated with changes in bond lengths and bond angles, and $\Delta V^{\ddagger}_{solv}$, the solvational volume change associated with changes in electrostriction during the activation process. Schematic representations of these contributions for typical bond formation and bond cleavage processes are given in Fig. 2. It is, of course, the $\Delta V^{\ddagger}_{intr}$ contribution that is the mechanistic indicator in terms of changes in bond lengths and angles during activation. In reactions with large changes in electrostriction, $\Delta V^{\ddagger}_{solv}$ may be even larger than $\Delta V^{\ddagger}_{intr}$ and can in fact counteract and swamp this contribution. Consequently, these two contributions should be separated in order to extract realistic values for the mechanistic indicator $\Delta V^{\ddagger}_{intr}$.

C. HIGH PRESSURE KINETIC TECHNIQUES

(i) Pressurizing system

The range of pressures available to industry and science covers more than 20 decades, for which a variety of gauges and devices are used to define the pressure scale [2,24]. Only about three decades of this pressure range fall in the kinetic high pressure range. The most common units used to express pressure are the megapascal (MPa), atmosphere, bar and pounds force per square inch (psi). Of these, the megapascal is the IUPAC approved unit. These units are related as shown below:

$$1 \text{ bar} = 0.1 \text{ MPa} = 0.986 \text{ atm} = 14.5 \text{ psi} \qquad (6)$$

Pressures up to 300 MPa can easily be attained with a manual hydraulic pump without the necessity of a pressure intensifier. The general scheme of a high pressure apparatus is shown in Fig. 3. The system consists of a hydraulic pump, pressure gauge, intensifier (optional), separator unit (to change pressurizing medium) and various valves and reservoirs. Pressure is obtained through mechanical compression of a hydraulic liquid such as oil or other suitable organic liquid such as *n*-heptane. In the case of direct optical measurements through the high pressure cell, it is often convenient to use water as a pressurizing medium. In such cases a separator unit is required to transmit the pressure from one medium to the other. For this purpose, either a spring-loaded piston or a Teflon tube (finger) is usually used. In the latter case the inner cylinder is filled with water and surrounded by the medium used in the hydraulic pump. In general, Viton O-rings are employed to seal the various parts for pressures up to 300 MPa at ambient temperature. At higher temperatures, or when the clearance between the surfaces to be sealed is large, metal wedge rings are used. The insertion of a

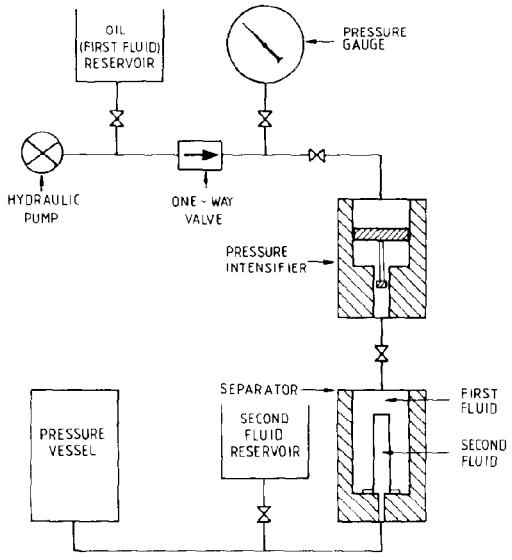

Fig. 3. Schematic drawing of a high pressure apparatus [23].

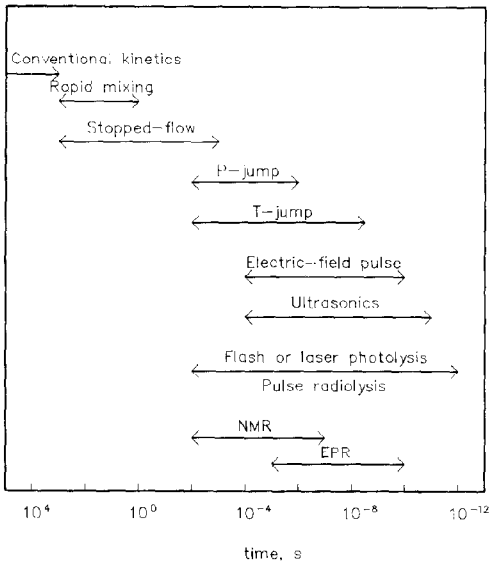

Fig. 4. Applicability of high pressure kinetic techniques for different time ranges.

one-way valve allows the hydraulic pump to be refilled without a significant drop in pressure in the system. Compressed inert gas may also be used to pressurize the system [25], although this requires special safety precautions compared with those required when working with compressed liquids. For instance, water at 100 MPa contains a stored energy of 72 J mol^{-1} compared with a value of 10^5 J mol^{-1} for an ideal gas under such conditions.

A detailed description of pressure generators, pressure intensifiers, materials for pressure vessels, pistons, seals, windows and a list of firms supplying such equipment is given elsewhere [2,24]. In the following sections, we present a systematic coverage of the various types of high pressure kinetic instrumentation used in mechanistic studies in coordination chemistry. Most of these instruments are usually home-made and constructed by the instrument shops of the laboratories involved. For more detailed information, readers are advised to contact the individual groups directly. The reported instrumentation enables kinetic measurements to be made over a wide range of time scales, i.e. from days and hours to microseconds and nanoseconds. A schematic presentation of the kinetic methods used as a function of time scale is given in Fig. 4.

(ii) Equipment for the study of slow reactions

Slow reactions can be performed either in a batch reactor (autoclave) equipped with a sampling valve or in situ in a high pressure cell using spectrophotometric or conductometric detection. Various systems have been reported that involve the withdrawal of aliquots from a pressurized reactor [26–30]. Contact between the sample and the steel vessel is avoided by placing the sample either in a polytetrafluoroethylene (PTFE) cylinder with a movable piston [28], or in a hypodermic syringe with a cut-off piston [29,30]. A typical example of such a reactor is presented in Fig. 5. This technique is highly suitable for slow and even extremely slow reactions at temperatures up to 140 °C. It has the disadvantage that large reaction volumes are needed to enable sufficient sampling of the reaction mixture. A compact version of this system has been constructed [31] in which two reaction components are placed in separated chambers and mixed after pressure and temperature equilibration.

The most commonly used method to monitor inorganic and organometallic reactions under pressure is in situ UV–visible spectrophotometry. A large variety of high pressure equipment has been used in conjunction with commercially available spectrophotometers [1,2,23,24,32–42]. In general, a sample cell is used within the high pressure cell to avoid contact with the cell and the pressurizing liquid. Such cells can range from PVC bags and Teflon tubes to glass cells with movable stoppers, since it must be possible to

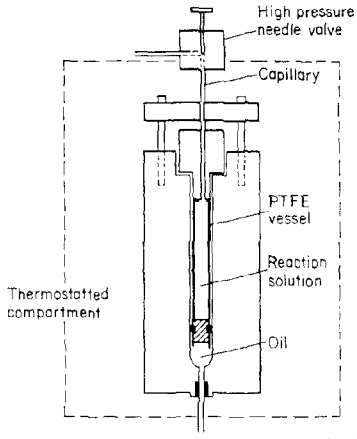

Fig. 5. High pressure reaction vessel with sampling valve [28].

transmit the pressure from the pressure medium to the sample. The volume decrease on compression depends on the kind of material and construction adopted as well as on the compressibility of the reaction medium, i.e. solvent. For instance, the isothermal compressibility of typical pressurizing mediums at 20 °C varies between 0.4×10^{-2} (Hg), 4.6×10^{-2} (H_2O) and 15.4×10^{-2} $kbar^{-1}$ (hexane). A typical example of a two-window high pressure cell is given in Fig. 6, and various types of glass and quartz sample

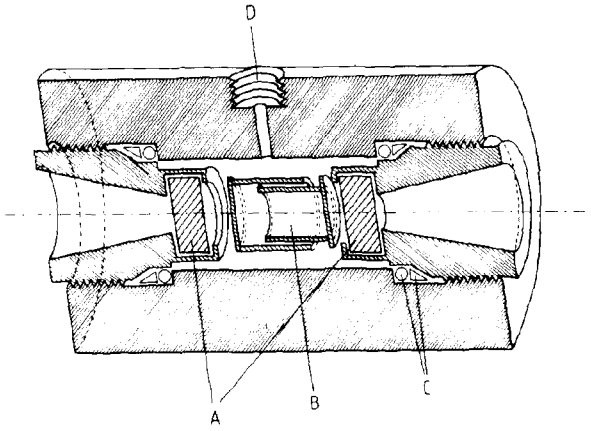

Fig. 6. A typical high pressure spectrophotometer cell [42]: A, sapphire or quartz windows; B, "pill-box" sample cell (Fig. 7); C, seals; D, hydraulic fluid inlet.

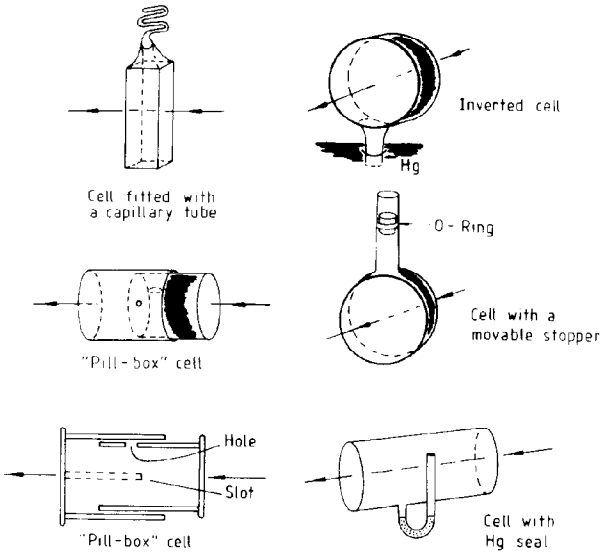

Fig. 7. Various types of optical sample cells [23].

cells are shown in Figs. 7 and 8. Similar high pressure cells have been constructed with three and four windows to study, for instance, photo-induced reactions [43]. Sapphire windows are usually employed in UV–visible spectrophotometry.

A very elegantly designed sample cell is the "pill-box" cell [37], which consists of two closely fitting quartz cylinders with windows and is filled with a syringe when the holes are aligned. The cell is sealed by turning one compartment 180°. A particular advantage of this cell is that the pressure is transmitted to the sample by the movable cylinders. The completely sealed optical cell (Fig. 8) was designed in our laboratories for the investigation of oxygen- and moisture-sensitive samples. In this case the deformable Teflon tube is used to transmit the pressure to the sample under investigation.

The pressure cells described can be thermostatted (± 0.1°C) and placed in the sample compartment of a double-beam spectrophotometer or connected to the latter with the aid of optical light leads. Such instrumentation is suitable for studying reactions with a half-life longer than 10 min, since that is the minimum time required to load the sample into the high pressure cell and to allow for temperature and pressure equilibration. Similar high pressure cells have been developed for IR and Raman spectroscopy [1–3]. However, in many cases the sample is in direct contact with the walls of the cell, which makes such instrumentation unsuitable for the study of inorganic

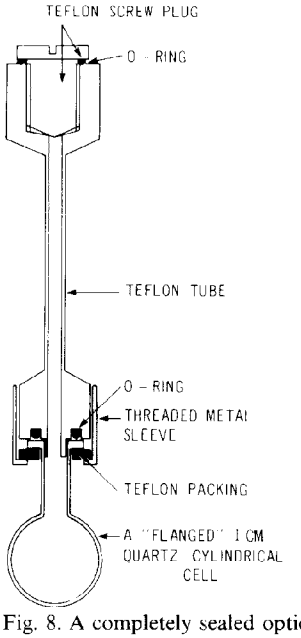

Fig. 8. A completely sealed optical cell [23].

and organometallic systems. Developments are presently in progress to design sample cells similar to the pill-box type that will enable the study of organometallic systems under high pressure using FT–IR techniques.

Typical examples of systems studied using the UV–visible technique include slow substitution reactions of square-planar and octahedral complexes. In general, substitution reactions of square-planar complexes with low spin d^8 configuration are characterized by the well-known two-term rate law (eqn. (7)):

$$k_{obs} = k_1 + k_2[Y] \tag{7}$$

where k_1 represents the solvolysis path and k_2 the direct ligand substitution path as shown in eqn. (8):

$$\begin{array}{l} ML_3X + S \xrightarrow{k_1} ML_3S + X \\ \qquad\qquad +Y \downarrow k_{an} \\ ML_3X + Y \xrightarrow{k_2} ML_3Y + X \end{array} \tag{8}$$

Most of the available kinetic data suggest that both reaction paths have the same associative character [44], although some arguments for dissociative activation in particular cases have also been reported [45,46]. Steric

TABLE 1

Kinetic parameters for the reaction [44] $Pd(L)Cl^+ + H_2O \xrightarrow[\text{slow}]{k_1} Pd(L)H_2O^{2+} + Cl^-$

$+I^- \downarrow$ fast

$Pd(L)I^+ + H_2O$

L	k_1 at 25 °C (s^{-1})	$\Delta H^{\ddagger}$ (kJ mol^{-1})	$\Delta S^{\ddagger}$ (J K^{-1} mol^{-1})	$\Delta V^{\ddagger}$ at 25 °C (cm^3 mol^{-1})
dien	43.8 ±0.5	43±3	−69±12	−10.0±0.6
1,4,7-Me_3dien	25.0 ±4.2	38±4	−87±15	−9.2±0.6
1,4,7-Et_3dien	10.0 ±0.1	41±5	−86±18	−10.8±1.0
1,1,7,7-Me_4dien	0.99±0.02	49±1	−79± 3	−13.4±1.9
1,1,4-Et_3dien	0.77±0.01	51±1	−76± 3	−14.5±1.2
1,1,4,7,7-Me_5dien	(2.76±0.04)×10^{-1}	50±1	−88± 3	−10.9±0.3
1,1,7,7,-Et_4dien	(2.1 ±0.4) ×10^{-3}	69±2	−67± 8	−14.9±0.2
4-Me-1,1,7,7-Et_4dien	(6.8 ±0.1) ×10^{-4}	66±7	−84±25	−14.3±0.6
1,1,4,7,7-Et_5dien	(6.7 ±0.1) ×10^{-4}	59±3	−106± 9	−12.8±0.8

hindrance, for instance, is one of the parameters that can hinder bond formation and force the system to react more dissociatively. Such a change-over in mechanism should clearly show up in the $\Delta V^{\ddagger}$ values. Data for a series of solvolysis reactions as a function of increasing steric hindrance, summarized in Table 1, demonstrate that the introduction of ethyl and methyl groups on the diethylenetriamine (dien) ligand significantly decreases k_1 with no substantial effect on either $\Delta S^{\ddagger}$ or $\Delta V^{\ddagger}$. The decrease in k_1 is ascribed to the more difficult attack of the solvent molecule as reflected in the increase in $\Delta H^{\ddagger}$. The average $\Delta V^{\ddagger}$ value of -12 ± 2 cm^3 mol^{-1} is close to the maximum value expected for the associative entry of a water molecule into the coordination sphere of an octahedral complex ion [47], but significantly more negative than the values reported for typical solvent exchange reactions of square-planar complexes, viz. −2.2 for $Pd(H_2O)_4^{2+}$ and −4.6 cm^3 mol^{-1} for $Pt(H_2O)_4^{2+}$ [48,49]. This probably means that solvolysis is accompanied by significant changes in electrostriction when the leaving group is anionic, i.e. during the formation of a trigonal bipyramidal intermediate. The $\Delta V^{\ddagger}$ values for neutral leaving groups (pyridine and NH_3) are very similar to those for solvent exchange and support the above arguments [50].

A volume profile for the solvolysis reaction can be constructed when $\Delta V^{\ddagger}$ for the k_1 path is combined with that for the reverse (anation) reaction [51]. Two typical examples are given in Fig. 9, from which it follows that the transition state has a substantially smaller value than either the reactant or product states, demonstrating the associative character of the substitution process.

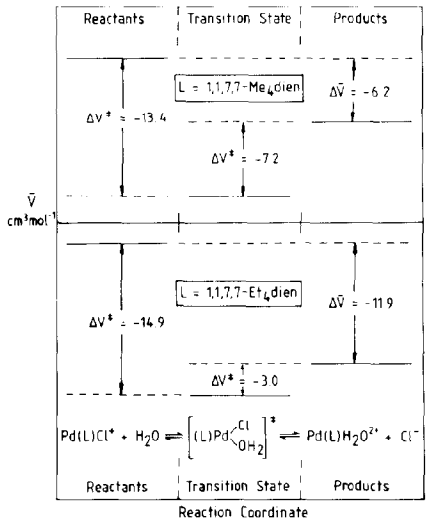

Fig. 9. Volume profiles for the reaction [51] $Pd(L)Cl^+ + H_2O \rightleftharpoons Pd(L)H_2O^{2+} + Cl^-$.

Substitution reactions of octahedral complexes, especially those of cobalt(III) and chromium(III), have received considerable attention from kineticists, and the definite assignment of the intimate mechanism remains a controversial issue. There is a long-standing argument about whether such reactions follow an I_a or I_d mechanism, and activation volume data have been used to settle the argument. In principle, the volume collapse during an I_a process (see Fig. 10) should result in a slightly negative $\Delta V^{\ddagger}$, compared with a slightly positive $\Delta V^{\ddagger}$ for an I_d process. The solvent exchange data for $Co(NH_3)_5H_2O^{3+}$ and $Cr(NH_3)_5H_2O^{3+}$ underline this expected trend with

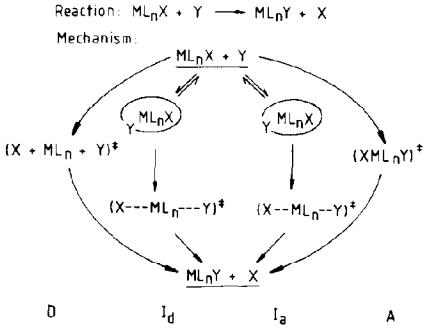

Fig. 10. Schematic representation of different types of substitution mechanisms [51].

$\Delta V^{\ddagger}$ values of $+1.2$ and -5.8 cm^3 mol^{-1} respectively [52,53]. However, aquation of the corresponding chloro complexes exhibits negative $\Delta V^{\ddagger}$ values in both cases [54], which are interpreted in terms of the I_d mechanism for the cobalt(III) complex and in terms of the I_a mechanism for the chromium(III) complex. The difference is ascribed to an increase in electrostriction owing to charge creation during breakage of the Co–Cl bond. Unambiguous mechanistic information can be obtained for such reactions only when the leaving group is neutral so that no major solvational changes occur. Data reported recently for the aquation of a series of complexes of the type $M(NH_3)_5X^{3+}$ (M = Co(III), Cr(III); X = neutral leaving group) demonstrate that $\Delta V^{\ddagger}$ is small throughout and positive for the cobalt(III) series but negative for the chromium(III) series [55,56]. Furthermore, these results are in excellent agreement with the solvent exchange data for the corresponding aqua complexes and underline the I_d and I_a character of the aquation process respectively.

Another technique used to follow slow reactions under pressure involves conductometry. Reactions in which a net change in ionic composition occurs can be monitored very effectively in this way. Various cell designs have been reported for such measurements under pressure [2,57–60]. Systems in which mercury is used as the pressure transmitting medium are in general unsuitable for studies in coordination chemistry. Furthermore, the platinum wire–glass seals used in some designs are fragile and often break under pressure. Therefore many high pressure conductivity cells are made of Teflon or Kel-F, and a typical design is presented in Fig. 11. A few important design aspects are indicated in detail in the figure. In general, this type of cell has the disadvantage that the cell constant varies with pressure, but since kinetic measurements are based on relative changes in conductivity, this does not affect the kinetic data.

An interesting example of a system studied with the aid of conductivity concerns the substitution reaction given in reaction (9), which was studied in a series of solvents:

$$\textit{trans}\text{-}Pt(py)_2(NO_2)Cl + py \rightarrow Pt(py)_3NO_2^{+} + Cl^{-} \qquad (9)$$

The aim of the study [60] was to separate $\Delta V^{\ddagger}_{intr}$ and $\Delta V^{\ddagger}_{solv}$. For reactions with a large change in dipole moment, $\Delta V^{\ddagger}_{solv}$ can be described by the solvent parameter q_p, which is obtained from the pressure derivative of the Kirkwood equation [61] given in eqn. (10):

$$q_p = \left[3/(2D+1)^2\right](\partial D/\partial P)_T \qquad (10)$$

The parameter q_p basically describes the solvent in terms of the pressure dependence of its dielectric constant. A single plot of $\Delta V^{\ddagger}$ vs. q_p should be linear with an intercept of $\Delta V^{\ddagger}_{intr}$, i.e. the volume change in a hypothetical

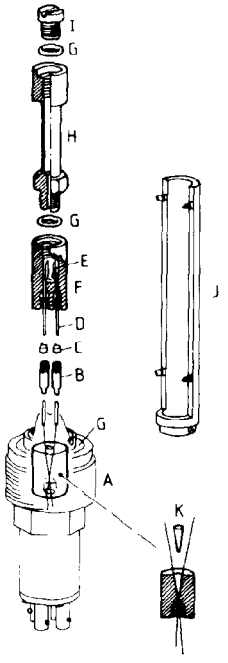

Fig. 11. High pressure conductivity cell [60]: A, plug of high pressure cell; B, hollow cylindrical Kel-F screw; C, Teflon cone; D, platinum wire lead; E, platinum electrode; F, Kel-F body; G, Viton O-ring; H, flexible Teflon tube; I, Teflon screw; J, aluminium holder; K, steel cone.

non-solvating medium, since $\Delta V^{\ddagger} = \Delta V^{\ddagger}_{\text{intr}} + \Delta V^{\ddagger}_{\text{solv}}$. Such a plot is presented in Fig. 12 for reaction (9) in four solvents, from which it follows that $\Delta V^{\ddagger}_{intr} = -7 \pm 1$ cm^3 mol^{-1}, consistent with an associative reaction mode. It

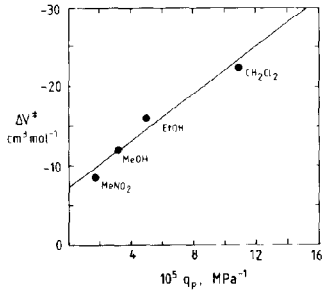

Fig. 12. The relationship between $\Delta V^{\ddagger}$ and q_p for the substitution of *trans*-Pt(py)$_2$(NO$_2$)Cl by pyridine [44].

follows that solvation effects play an important role in the overall value of $\Delta V^{\ddagger}$ as expressed by $\Delta V^{\ddagger} - \Delta V^{\ddagger}_{\text{intr}}$, which probably stems from the increased solvent interaction with the highly polar trigonal bipyramidal transition state [60].

(iii) Equipment involving mixing systems

The equipment discussed in the previous section allows the study of reactions with a half-life longer than 10 min. In order to perform faster reactions, i.e. in the minute, second and millisecond time range, it is essential to be able to initiate such reactions within the high pressure cell. With the aid of a mixing system, whether it is mechanical or a flow device, the reactants can be equilibrated at a desired temperature and pressure and then rapidly mixed to initiate the reaction. An example of a mechanical mixing system is presented in Fig. 13. It consists of two sample compartments separated by a Teflon membrane that can be broken on activating the mixing bar. Adequate mixing is obtained within 5 s, and the system is ideal for following reactions with half-lives of this order or longer. In the

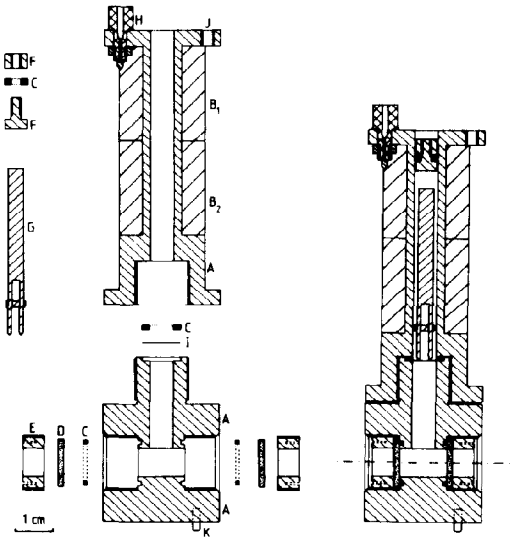

Fig. 13. Detailed drawing of the rapid mixing system [62]: A, Kel-F body; B, two coils; C, Teflon ring; D, window; E, Kel-F ring; F, Kel-F adjustable piston; G, soft-iron mixing bar; H, electrical connector; I, membrane; J, port for inserting rod; K, positioning pin.

instrument indicated the reaction is followed spectrophotometrically, although a similar set-up can also be used for conductometric detection.

An important breakthrough in the application of high pressure techniques in coordination chemistry was the development of high pressure stopped-flow equipment that enabled the study of fast reactions on a millisecond time scale. Heremans et al. [63] were the first to construct a very compact stopped-flow unit that fitted inside a high pressure cell (Fig. 14). A step motor was used to drive the sample syringes and the dead time of this instrument was reported to be about 40 ms at pressures up to 120 MPa. In a slightly modified version [64] (Fig. 15) the dead time of the instrument could be reduced to between 15 and 20 ms for pressures up to 100 MPa. A double-ring sealing system is used in the syringes, of which the outer ring is made out of a low friction resistance material. The tightness of the syringe seal can be adjusted. In these systems the receiver syringe is filled with solvent and used to flush the mixing cell before the reactant syringes are mounted onto the mixing block. In the latter design, a Durrum mixing jet is used between the reactant syringes and the observation chamber. Furthermore, the design is such that about 40 kinetic runs can be performed with one load of reactant solutions [64], which means that a complete pressure dependence can be covered. Merbach and coworkers [65,66] constructed a stopped-flow unit in which the sample syringes are driven by an external force as shown in Fig. 16. This set-up allows variation of the injected volume (typically 0.08 cm^3) and a maximum of 40 injections without refilling the syringes. Sasaki and coworkers [67,68] made use of a stopped-flow unit in which the sample and receiver syringes are placed in individual high pressure vessels, and mixing is accomplished by allowing the pressurized solutions to flow through the optical detection system. All the stopped-flow instruments discussed up to this point are such that the sample syringes are surrounded by a pressurizing medium. The danger does exist that the reactant solutions may be contaminated with small traces of the pressurizing medium, especially at high pressures. To avoid this complication, Tanaka and coworkers [69,70] designed a stopped-flow system in which the sample syringes are not immersed in the pressurizing medium. Their latest version of the instrument (Fig. 17) is characterized by a dead time of 3 ms for pressures up to 200 MPa. Balny et al. [71,72] constructed high pressure stopped-flow units with absorbance and fluorescence detection for cryoenzymologic studies at temperatures as low as $-30\,^{\circ}C$. The instrument was reported to have dead times of 5 ms at $20\,^{\circ}C$ and 50 ms at $-15\,^{\circ}C$.

There is at present a number of groups all over the world using such stopped-flow equipment which is also commercially available [73]. A variety of systems covering fast complex formation, ligand substitution, base hydrolysis, electron transfer, addition and elimination reactions have been

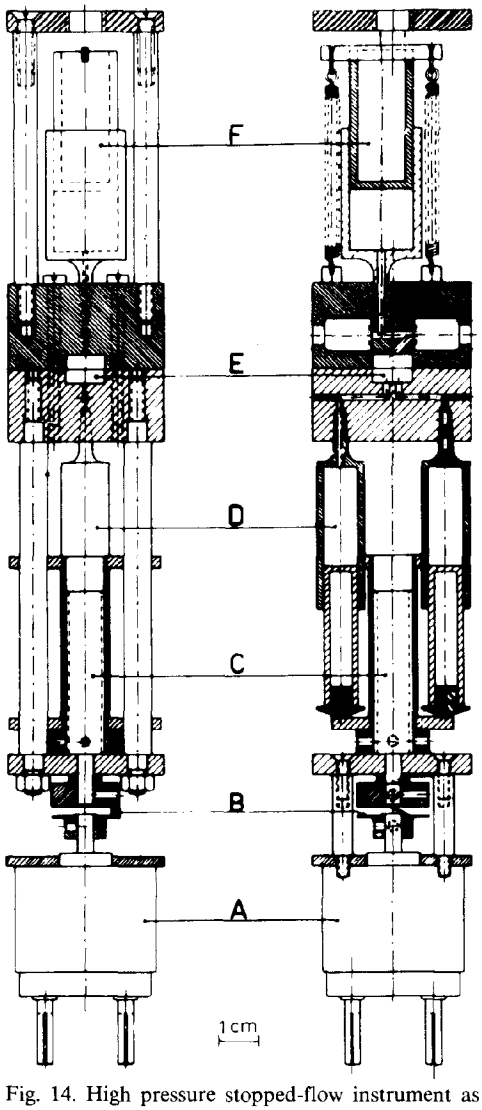

Fig. 14. High pressure stopped-flow instrument as used by Heremans et al. [63]: A, B, C, syringe driving mechanism: D, feed syringes; E, mixing chamber; F, waste syringe.

studied using this system [18,19]. In many cases it was possible to construct reaction volume profiles (similar to Fig. 9) and to contribute towards the understanding of the intimate mechanism. For instance, the base hydrolysis

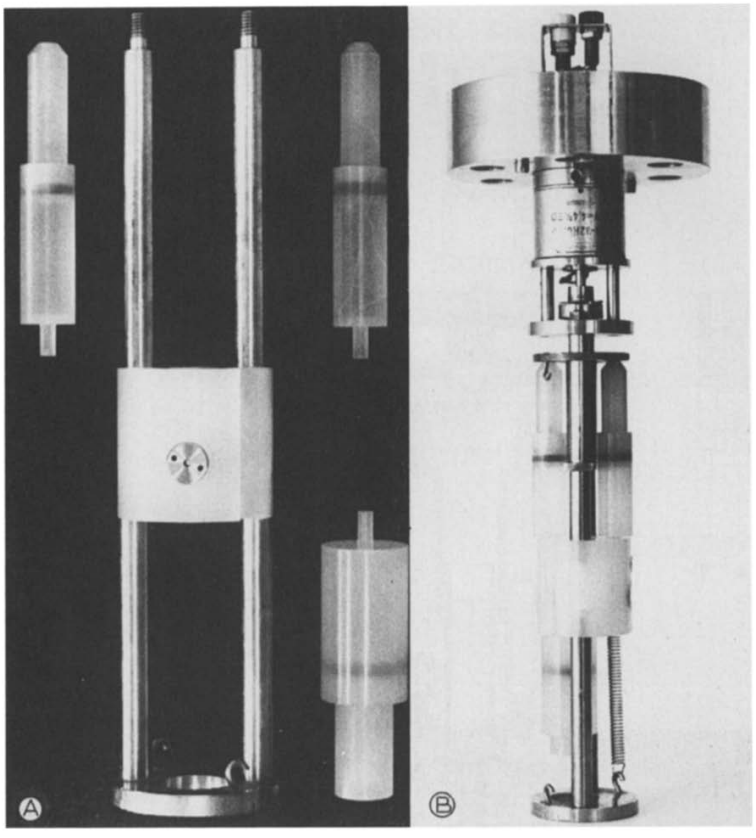

Fig. 15. High pressure stopped-flow instrument as used by van Eldik et al. [64]: A, essential components; B, complete unit.

reactions of a series of complexes of the type $Co(NH_3)_5X^{(3-n)+}$ are generally accepted to proceed according to an S_N1 CB mechanism as outlined in eqn. (11):

$$Co(NH_3)_5X^{(3-n)+} + OH^- \overset{K}{\rightleftharpoons} Co(NH_3)_4(NH_2)X^{(2-n)+} + H_2O$$

$$Co(NH_3)_4(NH_2)X^{(2-n)+} \xrightarrow{k} Co(NH_3)_4(NH_2)^{2+} + X^{n-}$$

$$Co(NH_3)_4(NH_2)^{2+} + H_2O \xrightarrow{\text{fast}} Co(NH_3)_5OH^{2+} \qquad (11)$$

The expected volume profile is given in Fig. 18. For this mechanism, $k_{obs} = kK[OH^-]$, such that $\Delta V^{\ddagger} = \Delta\bar{V}(K) + \Delta V^{\ddagger}(k)$, i.e. the sum of the reaction volume for conjugate base formation and the volume of activation

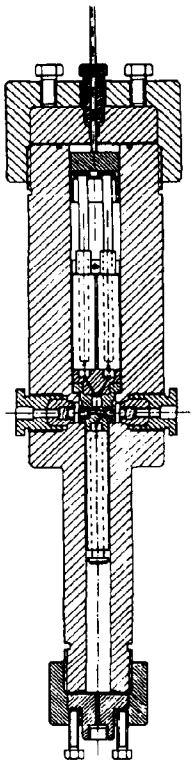

Fig. 16. High pressure stopped-flow instrument as used by Merbach and coworkers [66].

for the rate-determining dissociative reaction. Both these volume contributions are expected to depend on the nature of X^{n-}, since this species will determine the contribution arising from solvational changes due to charge creation. Typical values for $\Delta V^{\ddagger}$ (X^{n-}) are: $+40.2 \pm 0.5$ (dimethyl sulphoxide (DMSO)); $+31.0 \pm 0.8$ (NO_3^-); $+33.6 \pm 1.0$ (I^-); $+32.5 \pm 1.4$ (Br^-); $+33.0 \pm 1.4$ (Cl^-); $+26.4 \pm 1.0$ (F^-); and $+22.2 \pm 0.7$ (SO_4^{2-}) $cm^3\ mol^{-1}$ at 25 °C [74]. When these values are combined with $\Delta \bar{V}$ data for the overall process, it is possible to estimate the partial molar volume of the five-coordinate intermediate $Co(NH_3)_4NH_2^{2+}$. A similar treatment of the data for the base hydrolysis reactions of a series of monoalkyl-substituted complexes of the type *cis*- and *trans*-$Co(NH_3)_4(NH_2R)Cl^{2+}$ [75] indicated that the partial molar volume of the five-coordinate intermediate $Co(NH_3)_3(NH_2R)(NH_2)^{2+}$ increased linearly with the size of R and corresponded closely to that for the hydroxy complexes. Such studies allow information to be obtained on the

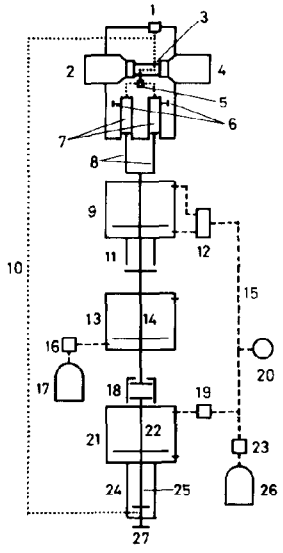

Fig. 17. Schematic diagram of the high pressure stopped-flow unit as used by Tanaka and coworkers [70] (dotted and broken lines represent pathways for solution and nitrogen gas respectively): 1, pressure sensor; 2, light source; 3, optical cell; 4, photomultiplier; 5, mixer; 6, high pressure cap; 7, high pressure syringe; 8, piston; 9, intensifier; 10, high pressure tube; 11, stopper and trigger; 12, change-over valve; 13, actuator; 14, rod; 15, gas tube; 16, solenoid valve; 17, gas reservoir; 18, coupler; 19, switching valve; 20, Bourdon gauge; 21, intensifier; 22, rod; 23, regulating valve; 24, high pressure cylinder; 25, piston; 26, gas reservoir; 27, high pressure valve.

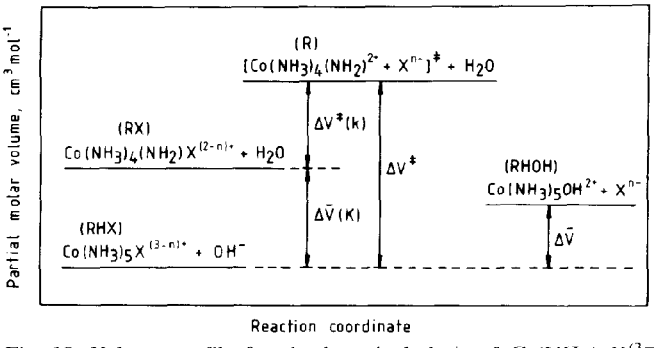

Fig. 18. Volume profile for the base hydrolysis of $Co(NH_3)_5X^{(3-n)+}$ according to the mechanism outlined in eqn. (11) [74].

size and volume of intermediate species in comparison with similar data for stable species.

High pressure stopped-flow techniques were also used to determine $\Delta V^{\ddagger}$ for substitution reactions of the triruthenium clusters $HRu_3(CO)_{11}^-$ and $Ru_3(CO)_{11}(CO_2CH_3)^-$. Under limiting conditions the loss of CO is rate determining and the corresponding values for $\Delta V^{\ddagger}$ are $+21.2 \pm 1.4$ cm^3 mol^{-1} and $+16 \pm 2$ cm^2 mol^{-1} respectively [76]. These values underline the dissociative nature of the process, notwithstanding the fact that slightly negative $\Delta S^{\ddagger}$ values were reported for both reactions. Such techniques have also been employed successfully in the study of electron-transfer reactions [13,93].

(iv) Equipment involving relaxation techniques

One of the most significant advances over the last decade has been the development of NMR, temperature jump (T-jump) and pressure-jump (P-jump) relaxation methods at pressures up to 300 MPa. The NMR techniques especially have opened up a wide research field in coordination chemistry and have contributed significantly to our understanding of fundamental chemical processes.

(a) NMR spectroscopy

The development of high pressure NMR techniques has been reviewed by Jonas [77–79], Merbach [8,9,80] and Moore [11]. In the following discussion we will focus on NMR techniques used to study liquids, since most of the work in coordination chemistry was performed in the liquid phase [81–92]. The instrumentation originally developed for spectrometers with electromagnets has been modified for use with superconducting magnets.

The material used to construct such NMR probes must be non-magnetic and of high mechanical strength: titanium and Be–Cu alloys, glass or quartz capillaries and sapphire give excellent results. In general, two approaches are used: in the first, glass tubing or quartz capillaries supporting pressures up to 200 MPa are used, with the advantage that the sample tubes fit directly into the probe of a narrow-bore magnet (Fig. 19 (a)). The main disadvantages are limitations in the pressure and temperature range, as well as poor NMR sensitivity due to small sample volumes. In the second approach, a probe head containing the high pressure cell with a built-in receiver coil replaces the commercial one (Fig. 19 (b)). The increase in line-width in the latter case, owing to non-spinning, is offset by a greater sensitivity due to an increase in sample volume. A typical probe head developed for wide-bore superconducting magnets is shown in Fig. 20. It consists of two aluminium supports. The lower one on the left contains a pressure cell made of Be–Cu

alloy, which can be used up to 250 MPa in a temperature range from −60 to 150 °C. The upper one contains the frequency adapter box. The internal components of the probe are also shown in Fig. 20. A special design has been reported for high pressure NMR studies of homogeneous catalysis in organometallic chemistry (Fig. 21).

High pressure NMR techniques have been used with great success in the study of solvent exchange and electron-transfer processes [8,9,80,93,94]. Solvent exchange reactions are of fundamental interest to understand the substitution behaviour of solvated metal ions. No net chemical reaction occurs during such a process, so that the overall $\Delta\overline{V}$ is zero and no major

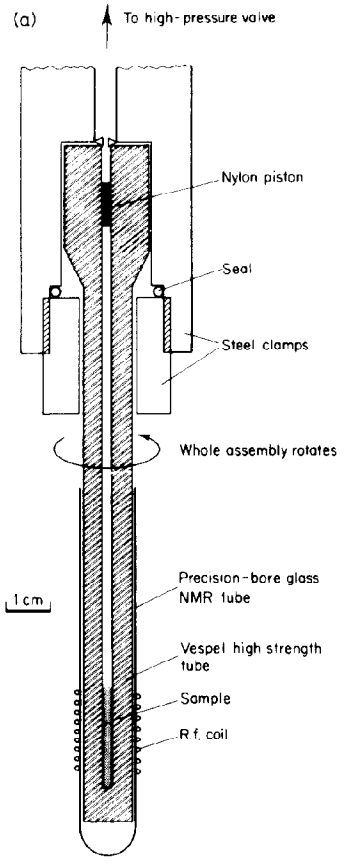

Fig. 19. High pressure NMR equipment as used by Merbach and coworkers [86]: (a) spinning high pressure sample tube; (b) static high pressure NMR probe.

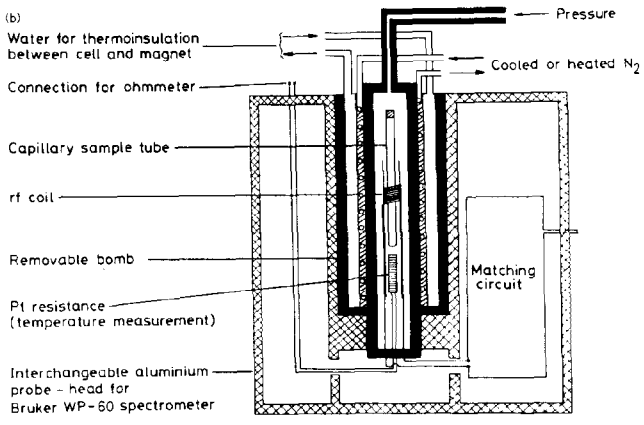

Fig. 19 (continued).

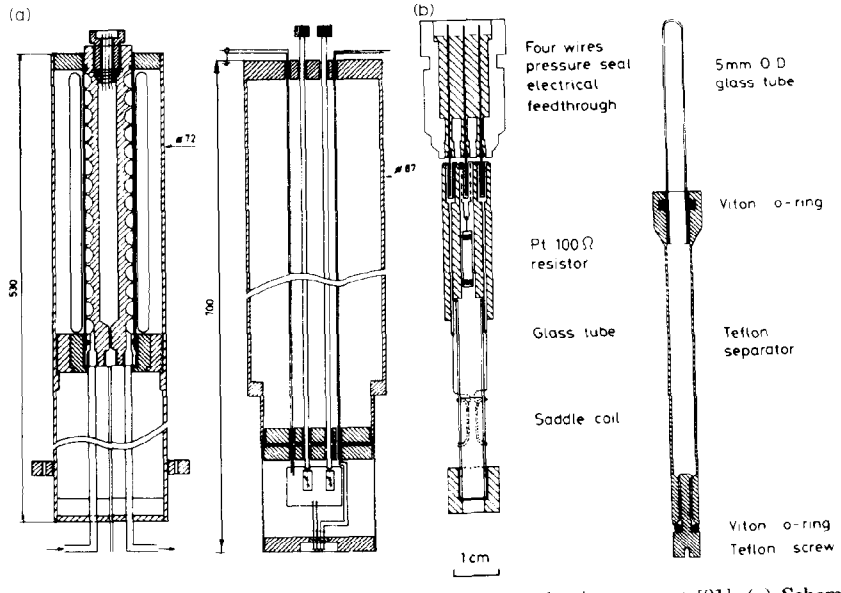

Fig. 20. Multinuclear high pressure probe for superconducting magnet [91]. (a) Schematic drawing of probe: lower aluminium support and high pressure cell (left); upper aluminium support and capacitive adapter box (right). (b) Internal components of probe: pressure seal and internal components of the cell (left); sample tube and separator assembly (right).

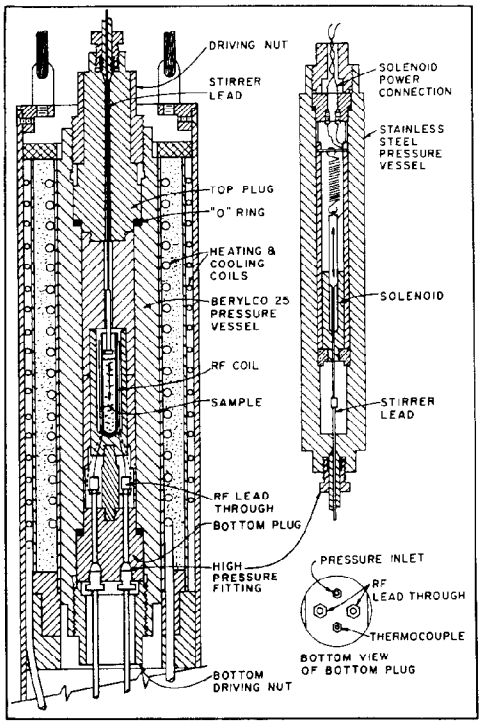

Fig. 21. High pressure probe for NMR studies of homogeneous catalysis [79].

change in electrostriction is expected to occur. This means that the reported $\Delta V^{\ddagger}$ data in fact represent $\Delta V^{\ddagger}_{intr}$ and therefore give immediate insight into the detail of the substitution mechanism. A summary of the $\Delta V^{\ddagger}$ data for solvent exchange of first row high spin transition metal ions (Table 2) exhibits a definite trend across the series. $\Delta V^{\ddagger}$ increases from negative to positive indicating a changeover in mechanism from associative (A) to dissociative (D) activation. The large positive and negative values could be indicative of limiting D and A mechanisms, whereas the small negative values (especially for Fe^{3+}) tend to favour an I_a mechanism. A similar changeover in mechanism was observed for solvent exchange of first row divalent metal ions (Table 3). The earlier members of the series are associatively activated (I_a) and the later members dissociatively activated (I_d). The data for Fe^{2+} are considered as a borderline case where a pure interchange mechanism (I) is operative. The data for dimethylformamide (DMF) exchange are significantly more positive (compared with those for the other solvents) for the larger metal ions, and it was suggested that steric hindrance

TABLE 2

Volumes of activation ($cm^3\ mol^{-1}$) for solvent S exchange on MS_6^{3+} of the first row transition metal series [a] [80]

M^{3+}	Sc	Ti	V	Cr	Fe	Ga
r_i (pm)	75	67	64	61	64	62
e_d	t_{2g}^0	t_{2g}^1	t_{2g}^2	t_{2g}^3	$t_{2g}^3 e_g^2$	$5_{2g}^6 e_g^4$
S						
H_2O		−12.1	−8.9	−9.6	−5.4	+5.0
DMSO				−11.3	−3.1	+13.1 [b]
DMF				−6.3	−0.9	+7.9 [b]
TMP [c]	−21.3					+20.7 [b]

[a] By NMR except for Cr^{3+} by isotopic labelling. [b] In CD_3NO_2 as diluent. [c] TMP, trimethylphosphate $(CH_3O)_3PO$.

may account for a more dissociatively activated transition state [96]. Structural and electronic factors have been suggested to account for the overall changeover observed in Table 3 [80]. Such mechanistic information could not have been obtained from conventional kinetic data, i.e. especially not from the values of $\Delta S^{\ddagger}$, since these are subject to large error limits due to the inherent extrapolation required to obtain this parameter, and the strong correlation with $\Delta H^{\ddagger}$ in statistical analyses.

(b) Temperature jump

Various high pressure T-jump instruments have been constructed, in which either laser excitation or an electrical discharge (Joule heating) is used to cause the temperature jump. Caldin et al. [97] first reported the construc-

TABLE 3

Volumes of activation ($cm^3\ mol^{-1}$) for solvent S exchange on MS_6^{2+} of the first row transition metal series by NMR [80]

M^{2+}	V	Mn	Fe	Co	Ni	Cu
r_i (pm)	79	83	78	74	69	(73) [a]
e_d	t_{2g}^3	$t_{2g}^3 e_g^2$	$t_{2g}^4 e_g^2$	$t_{2g}^5 e_g^2$	$t_{2g}^6 e_g^2$	$(t_{2g}^6 e_g^3)$
S						
H_2O	−4.1	−5.4	+3.8	+6.1	+7.2	
MeOH		−5.0	+0.4	+8.9	+11.4	+8.3
MeCN		−7.0	+3.0	+8.1	+8.5	
DMF		+2.0 [b]	+8.5	+6.7	+9.1	
NH_3					+5.9	

[a] Effective ionic radius. [b] Refs. 95 and 96.

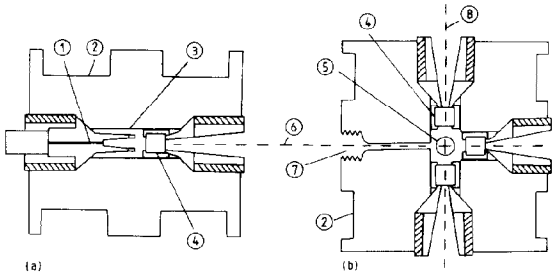

Fig. 22. High pressure laser T-jump apparatus as used by Caldin et al. [97] for (a) conductometric and (b) spectrophotometric detection: 1, conductance leads; 2, channel for thermostat water; 3, conductivity cell; 4, window; 5, optical cell; 6, laser beam axis; 7, high pressure connection; 8, optical detection axis.

tion of a high pressure laser T-jump apparatus for the study of fast reactions in the millisecond range at pressures up to 300 MPa. The advantage of a laser heating system is that the heating pulse can enter the cell through a transparent window, which simplifies the design of the instrument. A ruby or neodymium laser system was employed. They constructed two pressure vessels (Fig. 22): a one-window cell for conductometric detection and a three-window cell for spectrophotometric detection. In both cases a Kel-F (polychlorotrifluoroethylene) movable piston was used to transmit the pressure from the liquid pressurizing medium to the test solution. The instrument had a resolution time of 500 μs, which can be reduced to the microsecond time range with the more efficient laser equipment available today.

In the other high pressure T-jump instruments reported in the literature [39,98–102], an electrical discharge (Joule heating) was used to cause the temperature increase. In the instrument used by Grieger and coworkers [98] (Fig. 23) a double-layer plastic tube was used as the cell body, which also acted as a pressure transmitting device, with the result that the electrode distance varied with pressure. The system can be used for pressures up to 200 MPa with a dead time of between 10 and 20 μs. In the construction used by Jost [99] (Fig. 24), a gaseous pressurizing medium was used for pressures up to 400 MPa. The details of the construction show the way in which the electric leads are insulated. The dead time of this instrument was reported to be between 10 and 20 μs. In a later modification (Fig. 25) the sample was contained in a separated T-jump cell and the dead time of the instrument could be reduced to 50 ns [101]. Heremans [100] and Doss et al. [102] designed Joule-heating systems that are pressurized by liquids and in which a Teflon membrane in the T-jump cell is used to transmit the pressure. In both cases a special design for the high voltage feedthrough was adopted

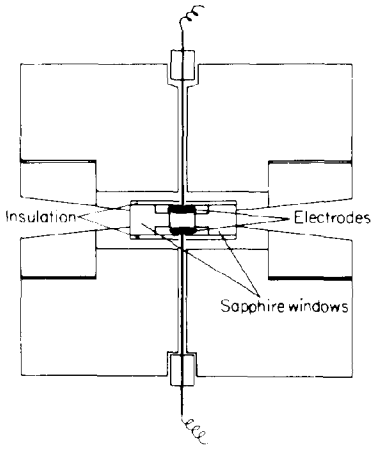

Fig. 23. High pressure T-jump cell as used by Grieger and coworkers [98].

(see Fig. 26 for more detail). Nimonic was used to construct the rather compact high pressure cell, and inert Kel-F was used for the T-jump cell. The inner cell is completely surrounded by the pressurizing liquid and has two quartz windows and two Teflon membranes. Typical heating times of about 10 μs and temperature jumps of 3°C for a discharge of 20 kV were reported [102].

T-jump instrumentation has been used with remarkable success in the study of fast complex formation reactions and processes of a bioinorganic nature [103–106]. For instance, $\Delta V^{\ddagger}$ values for the complex formation reactions of divalent first row transition metal ions, obtained using T-jump and stopped-flow methods [107–109], demonstrated that a mechanistic changeover similar to that reported for the solvent exchange reactions (Table 3) is also observed during complex formation (Table 4). In addition, such data enable the reaction volume profiles for such processes [54] to be constructed; a typical example is given in Fig. 27. It can be seen from this figure that the partial molar volume of the transition state is significantly lower than that of either the reactant or the product states, thus emphasizing the associative nature of the ligand substitution process in the case of manganese(II).

(c) Pressure jump

Only a few studies have employed P-jump techniques at elevated pressures [110–113]. Brower [110] was the first to perform such measurements at pressures up to 150 MPa and he used a deformable sample cell to separate the sample solution from the pressurizing medium. A schematic diagram of

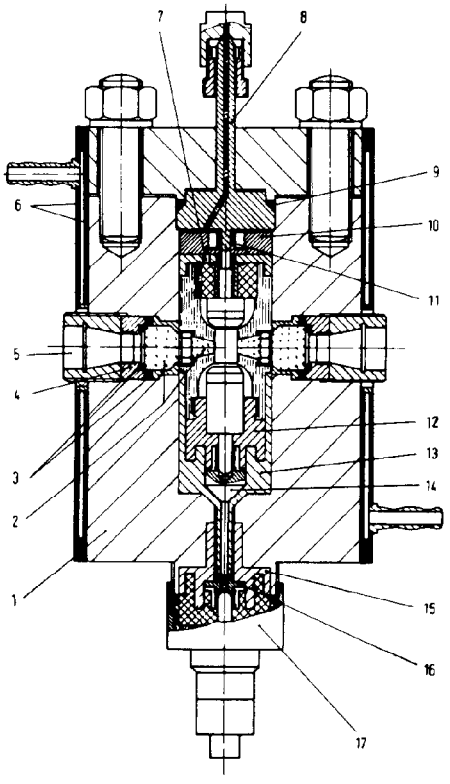

Fig. 24. High pressure T-jump cell as used by Jost [99]: 1, high pressure cell; 2, window; 3, seal; 4, pressure ring; 5, window holder; 6, thermostatted jacket; 7, gas entrance; 8, connection for compressor; 9, Bridgman seal; 10, spacer; 11, earth connector; 12, electrode holder; 13, nylon holder; 14, high voltage electrode; 15, nylon insulation; 16, adjustable seal; 17, high voltage plug from condensator.

the system used by Inoue et al. [113] is given in Fig. 28. The main improvement involves the usage of a pressure reservoir above the brass diaphragm. A pressure jump of 13 MPa is initiated by bursting this diaphragm. In general, such systems can be employed for the study of fast complex formation reactions that are accompanied by large volume changes, so that a pressure jump will initiate a relaxation process.

(v) Equipment for photochemical and photophysical measurements

Photochemical and photophysical measurements at elevated pressures include the determination of quantum yields for chemical and physical

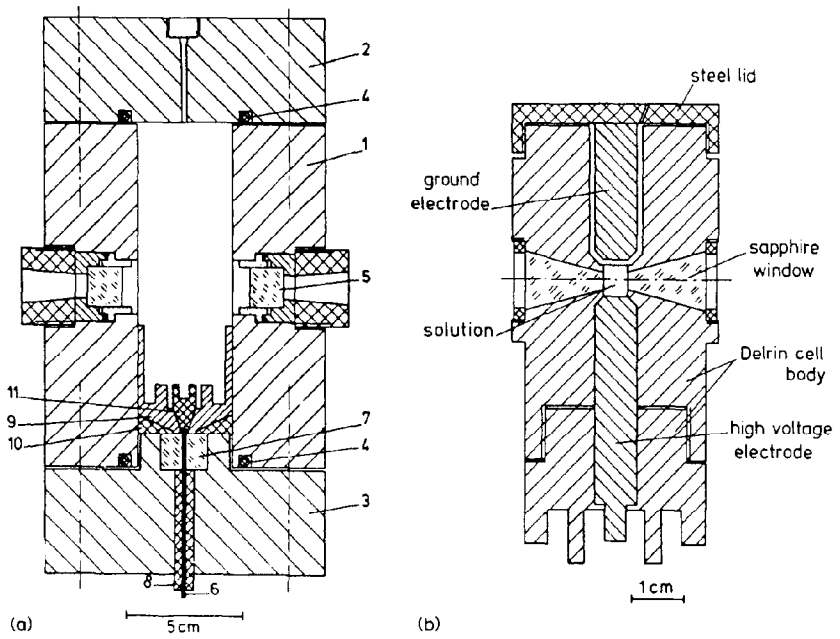

Fig. 25. High pressure T-jump cell as used by Liphard [101]. (a) High pressure cell: 1, autoclave; 2, 3, sealing caps; 4, O-ring; 5, sapphire window; 6, electrical feedthrough; 7, synthetic sapphire rod; 8, polyethylene bushing; 9, Delrin beaker; 10, Nimonic ring; 11, Inconel pin. (b) T-jump cell.

processes, as well as the measurement of excited state lifetimes and spectral properties as a function of pressure [16,114–116]. Details of such measurements on coordination complexes are reported in the literature [117–120]. In principle, high pressure cells with two to four optical windows (similar to that in Fig. 6) can be used for such measurements. Various sample cells can be used (see Figs. 7 and 8), of which the pill-box arrangement has proved to be very popular. For irradiation over longer periods of time, the sample solution is stirred magnetically using a Teflon-coated stirrer bar. Photochemical excitation is usually accomplished with the aid of monochromatic light from an xenon or a mercury lamp, or via a laser pulse. Time-resolved emission techniques have been used to measure excited state lifetimes for luminescent systems. In such cases, four windows in two perpendicular optical paths are located in the cell. Typical exciting light would be a pulse from an Nd/YAG laser which has been frequency doubled, tripled or quadrupled to give the wavelengths 532 nm, 355 nm or 266 nm respectively.

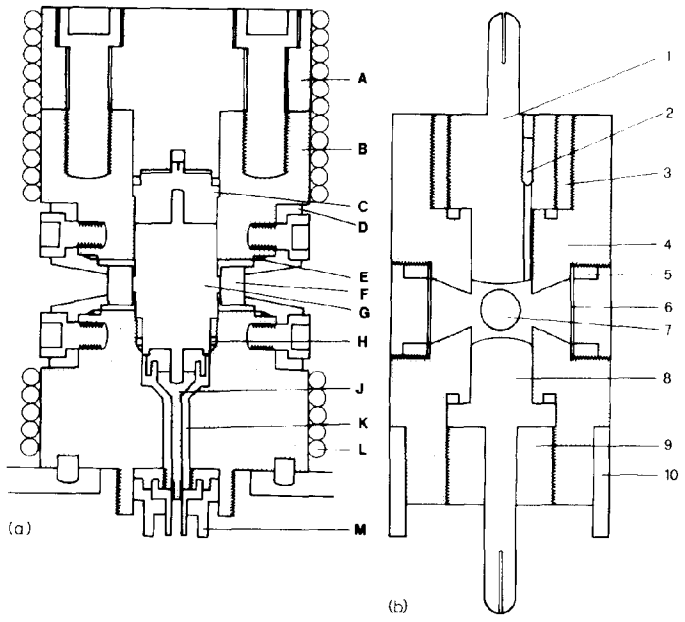

Fig. 26. High pressure T-jump cell as used by Doss et al. [102]. (a) High pressure cell: A, vessel lid; B, vessel body; C, steel piston; D, window support; E, Δ- and O-ring; F, sapphire window; G, space for T-jump cell; H, Δ- and O-ring; J, steel high voltage connecter; K, insulation material; L, circulation coil; M, high voltage plug. (b) T-jump cell: 1, upper electrode; 2, deaeration hole; 3, electrode thread support; 4, Kel-F cell body; 5, membrane support; 6, Teflon membrane; 7, optical window; 8, lower electrode; 9, threaded bold; 10, support ring.

TABLE 4

$\Delta V^{\ddagger}$ for the interchange of neutral and uninegative ligands on M^{2+} ions in water (from ref. 9)

Ligand [a]	V^{2+}	Mn^{2+}	Fe^{2+}	Co^{2+}	Ni^{2+}	Cu^{2+}	Zn^{2+}
H_2O	−4.1	−5.4	+3.8	+6.1	+7.2		
NH_3				+4.8	+6.0		
Imidazole					+11.0		
Isoquinoline					+7.4		
pada				+7.9	+7.1		
bpy		−1.2		+5.9	+5.3		
terpy		−3.4	+3.6	+4.1	+5.6		
SCN^-	−5.3						
Glycinate(1−)				+5	+7	+9	+4
Murexide(1−)					+8.7		

[a] pada = pyridine-2-azo-4-dimethylaniline; bpy = 2,2′-bipyridine; terpy = 2,2′ : 6′,2″-terpyridine.

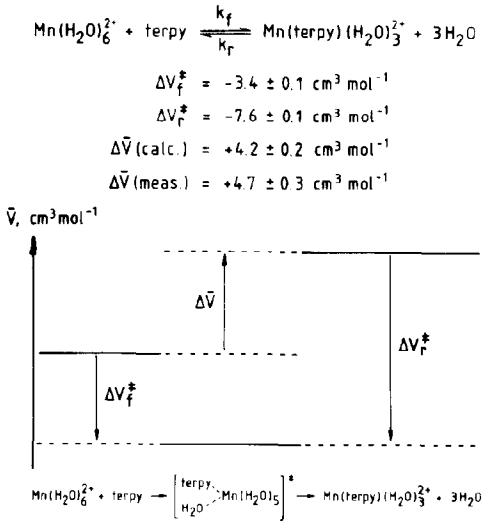

Fig. 27. Volume profile for a complex formation reaction of manganese(II) [108].

Emission is then detected along the perpendicular optical path using a fast photomultiplier tube and digital detection electronics.

To understand the effect of pressure on a photochemical reaction, it is of fundamental importance to have information on all the deactivation processes that affect the overall reaction and on their pressure dependences. Therefore $\Delta V^{\ddagger}$ calculated from the pressure dependence of the photochemical quantum yield is a composite quantity that reflects the volume changes associated with the photoreaction and non-radiative and radiative deactivation. A combined study of the pressure dependence of the photochemical

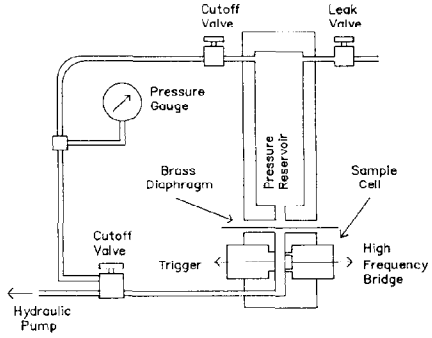

Fig. 28. Schematic diagram of a high pressure P-jump system as used by Inoue et al. [113].

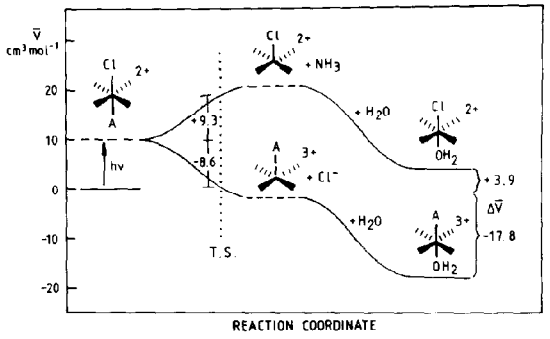

Fig. 29. Volume profile for the reaction [114]

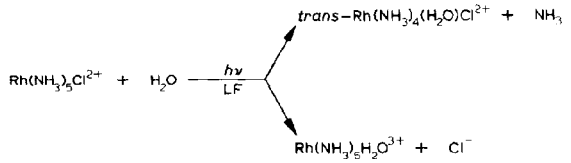

quantum yield and of the lifetime of the lowest excited state enables an analysis to be made in terms of the different contributing rate constants [117,121]. In this way it is possible to obtain mechanistic information on the nature of the photochemical process that may involve ligand substitution, isomerization or electron transfer [114]. A typical example of a volume profile for a ligand-field photosubstitution process is given in Fig. 29. It was assumed that the partial molar volume of the lowest excited triplet state is about 10 $cm^3\ mol^{-1}$ larger than that of the ground state species. The overall volume profiles are in line with a dissociatively activated mechanism and the significant increase in electrostriction accounts for the volume decrease observed during the photosolvolysis of the halide ligand. In a similar way, unique mechanistic information could be obtained on the non-radiative deactivation process in such systems [16].

Another interesting example concerns the linkage isomerization of $Co(en)_2(NH_2CH_2CH_2OSO)^{2+}$ which goes from S- to O-bonding photochemically (LMCT) and from O- to S-bonding thermally. These processes exhibit contrasting pressure dependences (Fig. 30) and lead to the overall volume profile shown in Fig. 31. The suggested mechanism involves a biradical-type ring-opening reaction for the photochemical process compared with the thermal ring opening that is accompanied by significant charge creation and an increase in electrostriction. The latter effect mainly accounts for the large volume difference between the photochemical and

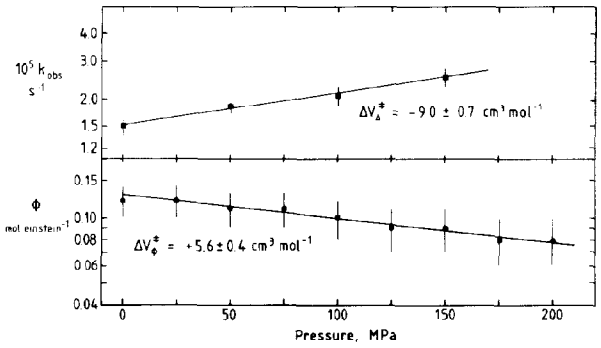

Fig. 30. Pressure dependences of the quantum yield for the forward reaction and the rate constant for the thermal back reaction in the overall process [122] $Co(SOON)^{2+} \underset{\Delta}{\overset{h\nu,\,CT}{\rightleftharpoons}} Co(OSON)^{2+}$.

thermal transition states. Detailed studies on photophysical deactivation processes have clearly demonstrated the large difference in volume between ligand-field (LF) and charge transfer (CT) excited states, for which the latter is close to that of the ground state species [120,123]. In many of the investigated systems, pressure is the only physical parameter available for obtaining insight into the mechanisms of the excited state species [114].

(vi) Other instrumentation

An apparatus for high pressure kinetic studies in liquid ammonia from −40 to +150 °C has been constructed and details are given elsewhere [124]. In addition, a very compact, transportable and multipurpose high pressure unit, complete with a four-window cell, was constructed to perform high

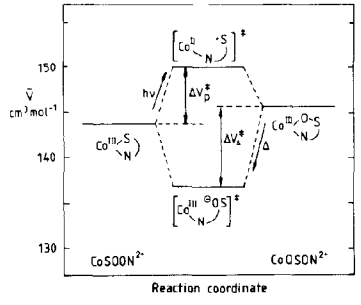

Fig. 31. Volume profile for the system [122] $Co(SOON)^{2+} \underset{\Delta}{\overset{h\nu,\,CT}{\rightleftharpoons}} Co(OSON)^{2+}$.

pressure kinetic measurements at other locations [125]. This system was, for instance, used to investigate the substitution behaviour of organometallic transients produced via flash photolysis [126].

Various instruments have been developed to determine reaction volumes from dilatometric and density measurements. These data are essential in order to construct volume profiles or to control reaction volumes determined from the pressure dependence of an equilibrium constant. Typical examples of dilatometers used to study slow as well as fast reactions are shown in Fig.

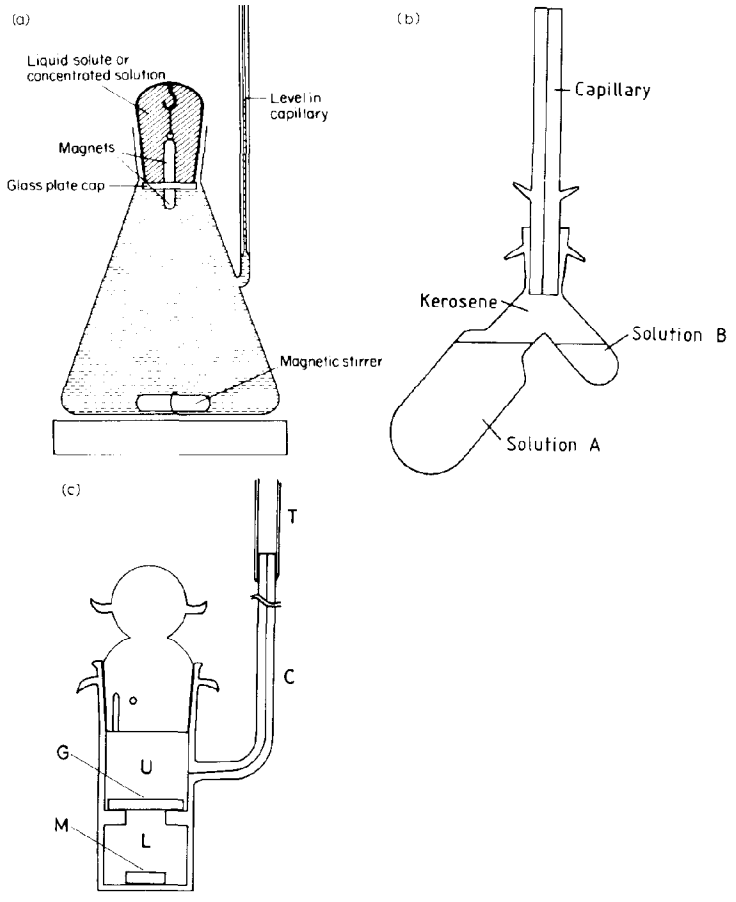

Fig. 32. Different types of dilatometers. (a) System used by Eckert et al. [2,127]. (b) Carlsberg dilatometer [128,129]. (c) Hashitani dilatometer [130]: G, glass plate; M, magnet; U, upper compartment; L, lower compartment.

32. After temperature equilibration, the separation between the two sample compartments is disturbed magnetically or by inverting the dilatometer, and the change in height of the liquid level in the capillary is recorded after completion of the reaction. The most convenient method to determine the partial molar volume of a species in solution is with the aid of an accurate, direct-reading densitometer that operates on the principle of a tuning fork. The frequency of the latter is determined by the density of the solution [131 133].

D. CONCLUDING REMARKS

The high pressure kinetic equipment discussed in the previous sections enables investigation of a wide range of reactions and systems in coordination chemistry [18]. The mechanistic information obtained adds a further dimension to our kinetic approach and assists the assignment of a detailed mechanism. In many cases it has become a necessity for the realistic assignment of the underlying reaction mechanism. The exponential increase in activity in this area over the last decade [19] is expected to continue to the point where almost all laboratories carrying out kinetic studies in coordination chemistry will apply this technique to the same extent that temperature is used as a kinetic variable. Such information can also be applied directly to synthetic work where the application of pressure may favour a particular reaction path that produces a specific product or isomer. Alternatively, it may reduce the reaction time or lower the reaction temperature to the point where unwanted side reactions are negligible.

Developments that may occur in the future could involve the application of pulsed-flow and combined stopped-flow–NMR techniques at elevated pressures. Areas of coordination chemistry that will receive more attention will be especially of an organometallic and a bioinorganic nature, with emphasis on homogeneous catalysis. Possible application in the area of radiation-induced reactions is under consideration. Finally, more developments can be expected in the application of significantly higher pressures (up to 10000 MPa) in mechanistic studies, where solvational changes are drastically reduced [134].

ACKNOWLEDGEMENTS

The authors gratefully acknowledge continued financial support from the Deutsche Forschungsgemeinschaft, the Fonds der Chemischen Industrie, and the Max-Buchner Forschungsstiftung.

REFERENCES

1 H. Kelm (Ed.), High Pressure Chemistry, Reidel, Dordrecht, 1978.
2 N. Isaacs, Liquid Phase High Pressure Chemistry, Wiley, Chichester, 1981.
3 R. van Eldik and J. Jonas (Eds.), High Pressure Chemistry and Biochemistry, Reidel, Dordrecht, 1987.
4 D.A. Palmer and H. Kelm, Coord. Chem. Rev., 36 (1981) 89.
5 T.W. Swaddle, Rev. Phys. Chem. Jpn., 50 (1980) 230.
6 T.W. Swaddle, in D.B. Rorabacher and J.F. Endicott (Eds.), Mechanistic Aspects of Inorganic Reactions, ACS Symposium Series, 198 (1982) 39.
7 T.W. Swaddle, Adv. Inorg. Bioinorg. Mech., 2 (1983) 95.
8 A.E. Merbach, Pure Appl. Chem., 54 (1982) 1479.
9 A.E. Merbach, Pure Appl. Chem., 59 (1987) 161.
10 M.J. Blandamer and J. Burgess, Pure Appl. Chem., 55 (1983) 55.
11 P. Moore, Pure Appl. Chem., 57 (1985) 347.
12 S.S. Batsanov, Usp. Khim., 55 (1986) 579.
13 R. van Eldik, Angew. Chem. Int. Ed. Engl., 25 (1986) 673.
14 R. van Eldik, Comments Inorg. Chem., 5 (1986) 135.
15 R. van Eldik, in M. Twigg (Ed.), Mechanisms of Inorganic and Organometallic Reactions, 3 (1985) 399; 4 (1986) 433; 5 (1988) 377.
16 J. DiBenedetto and P.C. Ford, Coord. Chem. Rev., 64 (1985) 361.
17 J.F. Endicott and C.K. Ryu, Comments Inorg. Chem., 6 (1987) 91.
18 R. van Eldik (Ed.), Inorganic High Pressure Chemistry: Kinetics and Mechanisms, Elsevier, Amsterdam, 1986.
19 R. van Eldik, T. Asano and W.J. le Noble, Chem. Rev., in press.
20 J. Jonas, Acc. Chem. Res., 17 (1984) 74.
21 J. Schroeder and J. Troe, Chem. Phys. Lett., 116 (1985) 453.
22 R. van Eldik, in R. van Eldik (Ed.), Inorganic High Pressure Chemistry: Kinetics and Mechanisms, Elsevier, Amsterdam, 1986, Chap. 8.
23 R. van Eldik, in R. van Eldik (Ed.), Inorganic High Pressure Chemistry: Kinetics and Mechanisms, Elsevier, Amsterdam, 1986, Chap. 1.
24 P.L.M. Heydemann, in H. Kelm (Ed.), High Pressure Chemistry, Reidel, Dordrecht, 1978, p. 1.
25 A. Jost, Ber. Bunsenges. Phys. Chem., 79 (1975) 850.
26 E. Whalley, Adv. Phys. Org. Chem., 2 (1964) 93.
27 A.R. Osborn and E. Whalley, Can. J. Chem., 39 (1961) 1094.
28 N.S. Isaacs and E. Rannala, J. Chem. Soc., Perkin Trans. 2, (1978) 709.
29 Y. Kondo, H. Tojima and N. Tokuru, Bull. Chem. Soc. Jpn., 40 (1967) 1408.
30 Y. Kitamura, T. Itoh and M. Takeuchi, Inorg. Chem., 25 (1986) 3887.
31 R.A. Grieger and C.A. Eckert, Trans. Faraday Soc., 66 (1970) 2579.
32 K.E. Weale, Chemical Reactions at High Pressures, Spon, London, 1967.
33 E.K. Fleischmann, E.G. Conze, D.R. Stranks and H. Kelm, Rev. Sci. Instrum., 45 (1974) 1427.
34 C.O. Leiber and A. Weller, Chem.-Ing. Tech., 39 (1967) 563.
35 F. Tanaka, M. Sasaki and J. Osugi, Rev. Phys. Chem. Jpn., 41 (1971) 18.
36 S.D. Hamann and M. Linton, J. Chem. Soc., Faraday Trans. 1, 70 (1974) 2239.
37 W.J. le Noble and R. Schlott, Rev. Sci. Instrum., 47 (1976) 770.
38 E.U. Franck, in H. Kelm (Ed.), High Pressure Chemistry, Reidel, Dordrecht, 1978, p. 221.

39 H. Lentz and S.O. Oh, High Temp.-High Pressures, 7 (1975) 91.
40 H.B. Tinker and D.E. Morris, Rev. Sci. Instrum., 43 (1972) 1024.
41 P. Figuiere, M. Ghelfenstein and H. Szwarc, High Temp.-High Pressures, 6 (1974) 61.
42 W.J. le Noble and H. Kelm, Angew. Chem. Int. Ed. Engl., 19 (1980) 841.
43 M. Spitzer, F. Gärtig and R. van Eldik, Rev. Sci. Instrum., in press.
44 M. Kotowski and R. van Eldik, in R. van Eldik (Ed.) Inorganic High Pressure Chemistry: Kinetics and Mechanisms, Elsevier, Amsterdam, 1986, Chap. 4.
45 S. Lanza, D. Minniti, P. Moore, J. Sachidis, R. Romeo and M.L. Tobe, Inorg. Chem., 23 (1984) 4428, and references cited therein.
46 G. Alibrandi, D. Minnitti, L.M. Scolaro and R. Romeo, Inorg. Chem., 27 (1988) 318.
47 T.W. Swaddle, Inorg. Chem., 22 (1983) 2663.
48 L. Helm, L.I. Elding and A.E. Merbach, Helv. Chim. Acta, 67 (1984) 1453.
49 L. Helm, L.I. Elding and A.E. Merbach, Inorg. Chem., 24 (1985) 1719.
50 M. Kotowski and R. van Eldik, Inorg. Chem., 25 (1986) 3896.
51 R. van Eldik, in R. van Eldik and J. Jonas (Eds.), High Pressure Chemistry and Biochemistry, Reidel, Dordrecht, 1978, p. 333.
52 H.R. Hunt and H. Taube, J. Am. Chem. Soc., 80 (1958) 2642.
53 T.W. Swaddle and D.R. Stranks, J. Am. Chem. Soc., 94 (1972) 8357.
54 R. van Eldik, in R. van Eldik (Ed.), Inorganic High Pressure Chemistry: Kinetics and Mechanisms, Elsevier, Amsterdam, 1986, Chap. 3.
55 G.A. Lawrance, Inorg. Chem., 21 (1982) 3687.
56 G.A. Lawrance and R. van Eldik, J. Chem. Soc., Chem. Commun., (1987) 1105.
57 S.B. Brummer and G.J. Hills, Trans. Faraday Soc., 57 (1961) 1816, 1823.
58 L.G. Blosser and H.S. Young, Rev. Sci. Instrum., 33 (1962) 1007.
59 J.B. Hyne H.S. Golinkin and W.G. Laidlaw, J. Am. Chem. Soc., 88 (1966) 2104.
60 M. Kotowski, D.A. Palmer and H. Kelm, Inorg. Chem., 18 (1979) 2555.
61 J.G. Kirkwood, J. Chem. Phys., 2 (1934) 351.
62 D.A. Palmer, R. Schmidt, R. van Eldik and H. Kelm, Inorg. Chim. Acta, 29 (1978) 261.
63 K. Heremans, J. Snauwaert and J. Rijkenberg, Rev. Sci. Instrum., 51 (1980) 806.
64 R. van Eldik, D.A. Palmer, R. Schmidt and H. Kelm, Inorg. Chim. Acta, 50 (1981) 131.
65 P.J. Nichols, Y. Ducommun and A.E. Merbach, Inorg. Chem., 22 (1983) 3993.
66 Y. Ducommun, P.J. Nichols, L. Helm, L.I. Elding and A.E. Merbach, J. de Phys., 45 C8 (1984) 221.
67 N. Takisawa, M. Sasaki, F. Amita and J. Osugi, Chem. Lett., (1979) 671.
68 M. Sasaki, F. Amita and J. Osugi, Rev. Sci. Instrum., 50 (1979) 1073.
69 S. Funahashi, K. Ishihara and M. Tanaka, Inorg. Chem., 20 (1981) 51.
70 K. Ishihara, S. Funahashi and M. Tanaka, Rev. Sci. Instrum., 53 (1982) 1231.
71 C. Balny, J.L. Saldana and N. Dahan, Anal. Biochem., 139 (1984) 178.
72 C. Balny, J.L. Saldana and N. Dahan, Anal. Biochem., 163 (1987) 309.
73 Hi-Tech Scientific Ltd., Churchfields, Salisbury, England. S. Lever and J. Crooks, American Laboratory–International Laboratory, October 1985.
74 Y. Kitamura, R. van Eldik and H. Kelm, Inorg. Chem., 23 (1984) 2038.
75 Y. Kitamura, R. van Eldik and C.R. Piriz Mac-Coll, Inorg. Chem., 25 (1986) 4252.
76 D.J. Taube, R. van Eldik and P.C. Ford, Organometallics, 6 (1987) 125.
77 J. Jonas, Adv. Magn. Reson., 6 (1973) 73.
78 J. Jonas, in H. Kelm (Ed.), High Pressure Chemistry, Reidel, Dordrecht, 1978, p. 65.
79 J. Jonas, in R. van Eldik and J. Jonas (Eds.), High Pressure Chemistry and Biochemistry, Reidel, Dordrecht, 1987, p. 193.
80 A.E. Merbach, in R. van Eldik and J. Jonas (Eds.), High Pressure Chemistry and Biochemistry, Reidel, Dordrecht, 1987, p. 311.

81 J. Jonas, Rev. Sci. Instrum., 43 (1972) 643.
82 J. von Jouanne and J. Heidberg, J. Magn. Reson., 7 (1972) 1.
83 H. Yamada, Chem. Lett., (1972) 747.
84 H. Yamada, Rev. Sci. Instrum., 45 (1974) 640.
85 J.G. Oldenziel and N.J. Trappeniers, Physica, 82A (1976) 565.
86 H. Vanni, W.L. Earl and A.E. Merbach, J. Magn. Reson., 29 (1978) 11.
87 W.L. Earl, H. Vanni and A.E. Merbach, J. Magn. Reson., 30 (1978) 571.
88 G. Voelkel, E. Lang and H.D. Luedemann, Ber. Bunsenges. Phys. Chem., 83 (1979) 722.
89 M.J. Sisley, Y. Yano and T.W. Swaddle, Inorg. Chem., 21 (1982) 1141.
90 A.R. Monnerat, P. Moore, K.E. Newman and A.E. Merbach, Inorg. Chim. Acta, 47 (1981) 139.
91 D.L. Pisaniello, L. Helm, P. Meier and A.E. Merbach, J. Am. Chem. Soc., 105 (1983) 4528.
92 H. Ilgen and J. von Jouanne, J. Magn. Reson., 59 (1984) 506.
93 T.W. Swaddle, in R. van Eldik (Ed.), Inorganic High Pressure Chemistry: Kinetics and Mechanisms, Elsevier, Amsterdam, 1986, Chap. 5.
94 L. Spiccia and T.W. Swaddle, Inorg. Chem., 26 (1987) 2265.
95 C. Cossy, L. Helm and A.E. Merbach, Helv. Chim. Acta, 70 (1987) 1516.
96 M. Ishii, S. Funahashi and M. Tanaka, Chem. Lett., (1987) 871.
97 E.F. Caldin, M.W. Grant, B.B. Hasinoff and P.A. Tregloan, J. Phys. E, 6 (1973) 349.
98 A.D. Yu, M.D. Waissbluth and R.A. Grieger, Rev. Sci. Instrum., 44 (1973) 1390.
99 A. Jost, Ber. Bunsenges. Phys. Chem., 78 (1974) 300.
100 K. Heremans, in H. Kelm (Ed.), High Pressure Chemistry, Reidel, Dordrecht, 1978, p. 311.
101 K.G. Liphard, Rev. Sci. Instrum., 50 (1979) 1089.
102 R. Doss, R. van Eldik and H. Kelm, Rev. Sci. Instrum., 53 (1982) 1592.
103 R. Doss and R. van Eldik, Inorg. Chem., 21 (1982) 4108.
104 E.F. Caldin, M.W. Grant and B.B. Hasinoff, J. Chem. Soc., Faraday Trans. 1, 68 (1972) 2247.
105 P. Martinez, R. Mohr and R. van Eldik, Ber. Bunsenges. Phys. Chem., 90 (1986) 609.
106 K. Heremans, in R. van Eldik (Ed.), Inorganic High Pressure Chemistry: Kinetics and Mechanisms, Elsevier, Amsterdam, 1986, Chap. 7.
107 R. Mohr and R. van Eldik, Inorg. Chem., 24 (1985) 3396.
108 R. Mohr, L.A. Mietta, Y. Ducommun and R. van Eldik, Inorg. Chem., 24 (1985) 757.
109 P.J. Nichols, Y. Ducommun and A.E. Merbach, Inorg. Chem., 22 (1983) 3993.
110 K.R. Brower, J. Am. Chem. Soc., 90 (1968) 5401.
111 M.W. Grant, J. Chem. Soc. Faraday Trans. 1, 69 (1973) 560.
112 K. Heremans, F. Centerick and J. Rijkenberg, Rev. Sci. Instrum., 51 (1980) 252.
113 T. Inoue, K. Koyima and R. Shimozawa, Chem. Lett., (1981) 259.
114 P.C. Ford, in R. van Eldik (Ed.), Inorganic High Pressure Chemistry: Kinetics and Mechanisms, Elsevier, Amsterdam, 1986, Chap. 6.
115 H.G. Drickamer, Ann. Rev. Phys. Chem., 33 (1982) 25.
116 H.G. Drickamer, in R. van Eldik and J. Jonas (Eds.), High Pressure Chemistry and Biochemistry, Reidel, Dordrecht, 1987, p. 263.
117 W. Weber, R. van Eldik, H. Kelm, J. DiBenedetto, Y. Ducommun, H. Offen and P.C. Ford, Inorg. Chem., 22 (1983) 623.
118 J.J. McCarvey, I. Lawthers, K. Heremans and H. Toftlund, J. Chem. Soc., Chem. Commun., (1984) 1575.
119 J. DiBenedetto, V. Arkle, H.A. Goodwin and P.C. Ford, Inorg. Chem., 24 (1985) 455.
120 M.L. Fetterolf and H.W. Offen, J. Phys. Chem., 89 (1985) 3320.

121 S. Wieland, J. DiBenedetto, R. van Eldik and P.C. Ford, Inorg. Chem., 25 (1986) 4893.
122 W. Weber, H. Maecke and R. van Eldik, Inorg. Chem., 25 (1986) 3093.
123 M.L. Fetterolf and H.W. Offen, J. Phys. Chem., 90 (1986) 1828.
124 S. Balt, J.Ph. Musch, W.E. Renkema and H. Ronde, J. Phys. E, 16 (1983) 82.
125 M. Spitzer, F. Gärtig and R. van Eldik, Rev. Sci. Instrum., in press.
126 H.H. Awad, G.R. Dobson and R. van Eldik, J. Chem. Soc., Chem. Commun., (1987) 1839.
127 J.R. McCabe, R.A. Grieger and C.A. Eckert, Ind. Eng. Chem. Fundam., 9 (1970) 156.
128 J. Rasper and W. Kauzmann, J. Am. Chem. Soc., 84 (1962) 1771.
129 K. Linderstroem-Lang and H. Lanz, C. R. Trav. Lab. Carlsberg, Ser. Chim., 21 (1938) 315.
130 M. Uemoto and T. Hashitani, J. Chem. Soc., Faraday Trans. 1, 81 (1985) 2333.
131 O. Krathy, H. Leopold and H. Stabinger, Z. Angew. Phys., 27 (1969) 273.
132 M.R.J. Dack, K.J. Bird and A.J. Parker, Aust. J. Chem., 28 (1975) 955.
133 R. Picker, E. Tremblay and C. Jolicoeur, J. Solution Chem., 6 (1977) 733.
134 P.P.S. Saluja, C. Cameron, M.A. Florino, A. Lavergne, G.E. McLaurin and E. Whalley, Rev. Sci. Instrum., 57 (1986) 2791.